

# Effect of increased stability of peptide-based coatings in the Casimir regime via nanoparticle doping

G. L. Klimchitskaya,<sup>1,2</sup> V. M. Mostepanenko,<sup>1,2,3</sup> and E. N. Velichko<sup>2</sup>

<sup>1</sup>*Central Astronomical Observatory at Pulkovo of the Russian Academy of Sciences, Saint Petersburg, 196140, Russia*

<sup>2</sup>*Institute of Physics, Nanotechnology and Telecommunications,*

*Peter the Great Saint Petersburg Polytechnic University, Saint Petersburg, 195251, Russia*

<sup>3</sup>*Kazan Federal University, Kazan, 420008, Russia*

We find that thin peptide films and coatings doped with metallic nanoparticles are more stable due to the role of electromagnetic fluctuations. It is shown that for the doped freestanding in vacuum peptide film the Casimir attraction becomes larger in magnitude. For dielectric substrates coated with peptide films, the nanoparticle doping leads to a wider range of film thicknesses where the Casimir pressure is attractive and to larger pressure magnitudes at the points of extremum. The doping of peptide coatings with magnetic nanoparticles preserves all the advantages of nonmagnetic ones and simultaneously imparts superparamagnetic properties to the coating which could extend significantly the application areas of bioelectronics.

It is common knowledge that thin films and coatings based on peptides, proteins and other biological polymers find increasing bioelectronic and biomedical applications [1, 2]. Peptides are the relatively short chains of amino acids linked by peptide bonds. These are nonmetallic materials which possess some electrical conductivity and enjoy wide use in optical and electronic devices, as well as in biomedical technologies, for creating thin film transistors, biomarkers, sensors, and biocompatible electrodes alternative to conventional devices based on the silicon technologies [3–9].

The most general requirements imposed upon peptide-based coatings are the stability, even in adverse conditions, reproducible diagnostic results, the ease of fabrication and, in medical applications, biocompatibility and non-toxicity [10–12]. In the last two decades, great progress has been made in developing miniature bioelectronic devices satisfying these requirements (see, for instance, Refs. [13–17]). In doing so, with decreasing the characteristic device dimensions to below a micrometer, the role of quantum effects and, specifically, the zero-point and thermal fluctuations of the electromagnetic field, increases in importance.

The fluctuation phenomena and their role in nanoscale science are the long-explored areas [18, 19]. Much experimental and theoretical attention has been paid to investigation of the fluctuation-induced van der Waals and Casimir forces between the boundary surfaces made of inorganic materials (see, e.g., Refs. [20–23] for a review). It was demonstrated that at separations below a micrometer these forces may exceed in magnitude the characteristic electric force and can be used as an actuator in micro- and nanoelectromechanical devices of the next generations.

These experimental and theoretical advances are largely based on the fundamental Lifshitz theory which allows calculation of the van der Waals and Casimir forces between surfaces with known frequency-dependent dielectric permittivities [20–24]. The Lifshitz theory was

also used to calculate the fluctuation-induced forces acting between varied in composition organic films [25–28] and the free energies of both freestanding in vacuum and deposited on substrates peptide films [29, 30]. It was shown that the free energy of peptide coating is a nonmonotonous function of the film thickness and may change its sign. However, the fluctuation-induced pressure in peptide films and coatings was not considered so far.

In this Rapid Communication, we investigate the pressure in peptide films and coatings in the Casimir regime (i.e., for film thicknesses below a micrometer), and find the effect of increased stability which arises via the nanoparticle doping. For this purpose, we calculate the Casimir pressure in the framework of the Lifshitz theory for the ordinary and doped with metallic nanoparticles peptide films and coatings. Both cases of nonmagnetic and magnetic nanoparticles are considered. In the latter case, the coating becomes superparamagnetic which is beneficial for various applications (the possibility for fabrication of peptide films with well distributed metallic nanoparticles was demonstrated in Ref. [31]). According to our results, the doping of a peptide coating with metallic nanoparticles leads to a larger in magnitude (negative) minimum value of the Casimir pressure which makes the coating more stable. Taking into consideration that stability is an essential feature required of peptide coatings, future prospects for the use of this effect are discussed.

We consider the three-layer system consisting of a vacuum and a doped peptide film of thickness  $a$  deposited on a nonmagnetic dielectric substrate. Separate layers of this system are described by the dielectric permittivities  $\varepsilon^{(0)} = 1$ ,  $\varepsilon^{(1)}(\omega)$ ,  $\varepsilon^{(2)}(\omega)$  and magnetic permeabilities  $\mu^{(0)} = 1$ ,  $\mu^{(1)}(\omega)$  and  $\mu^{(2)} = 1$ , respectively. The substrate is assumed to be thicker than  $2 \mu\text{m}$  in which case it can be replaced with a semispace in calculations of the Casimir pressure [32]. For a freestanding in a vacuum peptide film, one should put  $\varepsilon^{(2)}(\omega) = 1$ . The Casimir

pressure of the peptide coating (film) at temperature  $T$  is given by the Lifshitz theory

$$P(a) = -\frac{k_B T}{\pi} \sum_{l=0}^{\infty}{}' \int_0^{\infty} k p^{(1)}(i\xi_l, k) dk \quad (1)$$

$$\times \sum_{\alpha} \frac{1}{\left[ r_{\alpha}^{(1,0)}(i\xi_l, k) r_{\alpha}^{(1,2)}(i\xi_l, k) \right]^{-1} e^{2ap^{(1)}(i\xi_l, k)} - 1}.$$

Here,  $k_B$  is the Boltzmann constant,  $\xi_l = 2\pi k_B T l / \hbar$  with  $l = 0, 1, 2, \dots$  are the Matsubara frequencies, the prime on the sum in  $l$  divides the term with  $l = 0$  by two,  $k$  is the magnitude of the wave vector projection on the plane of peptide film, the sum in  $\alpha$  is over two independent polarizations of the electromagnetic field, transverse electric ( $\alpha = \text{TE}$ ) and transverse magnetic ( $\alpha = \text{TM}$ ), and

$$p^{(n)}(i\xi_l, k) = \sqrt{k^2 + \varepsilon^{(n)}(i\xi_l) \mu^{(n)}(i\xi_l) \frac{\xi_l^2}{c^2}}, \quad (2)$$

where  $n = 0, 1, 2$ .

Equation (1) also contains the reflection coefficients on the boundary planes between a film and a vacuum

$$r_{\text{TM}}^{(1,0)}(i\xi_l, k) = \frac{p^{(1)}(i\xi_l, k) - \varepsilon^{(1)}(i\xi_l) p^{(0)}(i\xi_l, k)}{p^{(1)}(i\xi_l, k) + \varepsilon^{(1)}(i\xi_l) p^{(0)}(i\xi_l, k)}, \quad (3)$$

$$r_{\text{TE}}^{(1,0)}(i\xi_l, k) = \frac{p^{(1)}(i\xi_l, k) - \mu^{(1)}(i\xi_l) p^{(0)}(i\xi_l, k)}{p^{(1)}(i\xi_l, k) + \mu^{(1)}(i\xi_l) p^{(0)}(i\xi_l, k)},$$

and between a film and a substrate

$$r_{\text{TM}}^{(1,2)}(i\xi_l, k) = \frac{\varepsilon^{(2)}(i\xi_l) p^{(1)}(i\xi_l, k) - \varepsilon^{(1)}(i\xi_l) p^{(2)}(i\xi_l, k)}{\varepsilon^{(2)}(i\xi_l) p^{(1)}(i\xi_l, k) + \varepsilon^{(1)}(i\xi_l) p^{(2)}(i\xi_l, k)},$$

$$r_{\text{TE}}^{(1,2)}(i\xi_l, k) = \frac{p^{(1)}(i\xi_l, k) - \mu^{(1)}(i\xi_l) p^{(2)}(i\xi_l, k)}{p^{(1)}(i\xi_l, k) + \mu^{(1)}(i\xi_l) p^{(2)}(i\xi_l, k)}. \quad (4)$$

Equation (1) has been extensively used to investigate the Casimir effect in inorganic (metallic and dielectric) films and coatings [33–38]. It allows computation of the Casimir pressure as a function of film thickness by the known quantities  $\varepsilon^{(n)}(i\xi_l)$  and  $\mu^{(1)}(i\xi_l)$ . In doing so, at room temperature the result depends only on  $\mu^{(1)}(0)$  [39].

An application of the same approach to peptide films is not a simple task. The point is that for typical peptides the optical data over the wide frequency range are not available. What is more, peptide films usually contain some volume fraction of a plasticizer whose role may be played by water [40, 41]. If the peptide film is doped with nanoparticles, this should be taken into account in its effective dielectric permittivity.

In Ref. [29] the dielectric permittivity of a model peptide  $\varepsilon^{(p)}(i\xi_l)$  along the imaginary frequency axis was composed from the imaginary parts of the permittivities of electrically neutral 18-residue zinc finger peptide in the microwave region [42] and of cyclic tripeptide RGD-4C in the region of ultraviolet frequencies [43]. The permittivity of water,  $\varepsilon^{(w)}(i\xi_l)$ , was used in the representation

of Ref. [44]. The molecules of the model peptide are assumed to have an irregular shape, be a few nanometers in size and randomly distributed in water. Under an assumption that a peptide film contains the volume fraction of water  $\Phi$ , the film dielectric permittivity,  $\varepsilon_{\Phi}^{(p)}(i\xi_l)$ , is then found from the mixing formula [45]

$$\frac{\varepsilon_{\Phi}^{(p)}(i\xi_l) - 1}{\varepsilon_{\Phi}^{(p)}(i\xi_l) + 2} = \Phi \frac{\varepsilon^{(w)}(i\xi_l) - 1}{\varepsilon^{(w)}(i\xi_l) + 2} + (1 - \Phi) \frac{\varepsilon^{(p)}(i\xi_l) - 1}{\varepsilon^{(p)}(i\xi_l) + 2}, \quad (5)$$

which is a consequence of the Clausius-Mossotti equation. The obtained dielectric permittivities  $\varepsilon_{\Phi}^{(p)}(i\xi_l)$  for  $\Phi = 0, 0.1, 0.25$ , and  $0.4$  as the functions of  $\xi$  are presented in Fig. 2 of Ref. [29]. It is seen that  $\varepsilon_0^{(p)}(i\xi_l) = \varepsilon^{(p)}(i\xi_l)$ .

Substituting  $\varepsilon^{(1)} = \varepsilon_{\Phi}^{(p)}$  and  $\mu^{(1)} = \varepsilon^{(2)} = 1$  in Eq. (1), we have computed the Casimir pressure in the freestanding in a vacuum undoped peptide film containing different volume fractions  $\Phi$  of water at  $T = 300$  K. The computational results are shown in Fig. 1 by the dashed line ( $\Phi = 0$ ) and by the following three black solid lines counted from top to bottom for  $\Phi = 0.1, 0.25$ , and  $0.4$ , respectively, as the functions of film thickness. As is seen in Fig. 1, the pressure is negative which corresponds to an attraction and makes film more stable.

Now we consider the peptide film containing the volume fraction  $\Phi$  of water and assume that it is then doped with Au nanoparticles of spherical shape occupying the volume fraction  $\beta$  of the obtained film. The dielectric permittivity of Au nanoparticles along the imaginary fre-

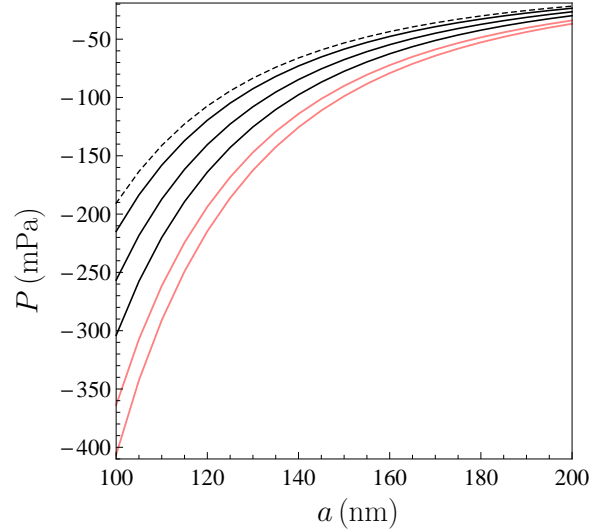


FIG. 1: The Casimir pressures in freestanding undoped peptide films (the dashed line is for a pure peptide and the following three black solid lines from top to bottom are for the films containing  $\Phi = 0.1, 0.25$ , and  $0.4$  fractions of water, respectively) and in doped with Au nanoparticles peptide films with  $\Phi = 0.4$  (the lowest and the next to it solid lines are for the films containing  $\beta = 0.05$  and  $0.03$  volume fractions of nanoparticles, respectively) are shown as the functions of film thickness at  $T = 300$  K.

quency axis  $\varepsilon_{\text{Au}}(i\xi_l)$  is found using the optical data for Au [46] and was extensively used in calculations of the Casimir force [21–23]. As a result, the dielectric permittivity of doped peptide film is given by the Maxwell-Garnet mixing formula [47]

$$\varepsilon_{\Phi,\beta}^{(p)} = \varepsilon_{\Phi}^{(p)} \left( 1 + \frac{3\beta X}{1 - \beta X} \right), \quad X = \frac{\varepsilon_{\text{Au}} - \varepsilon_{\Phi}^{(p)}}{\varepsilon_{\text{Au}} + 2\varepsilon_{\Phi}^{(p)}}. \quad (6)$$

Computations of the Casimir pressure are made at  $T = 300$  K for the doped freestanding peptide films using Eq. (1) where  $\varepsilon^{(1)} = \varepsilon_{\Phi,\beta}^{(p)}$ ,  $\mu^{(1)} = \varepsilon^{(2)} = 1$ ,  $\Phi = 0.4$ , and  $\beta = 0.03$  or  $0.05$ . The computational results are shown in Fig. 1 as the functions of film thickness by the lowest and next to it solid lines ( $\beta = 0.05$  and  $0.03$ , respectively). It is seen that these lines demonstrate much larger in magnitude Casimir pressures than the bottom black line which holds for an undoped film with  $\Phi = 0.4$ .

Now we turn our attention to the most interesting case from the practical standpoint, i.e., to peptide films deposited on a dielectric substrate. As a substrate material we use  $\text{SiO}_2$  glass [6] which dielectric permittivity  $\varepsilon^{(2)}(i\xi)$  has an accurate analytic representation [45]. First we calculate the Casimir pressure in an undoped coating using Eq. (1) where  $\varepsilon^{(1)} = \varepsilon_{\Phi}^{(p)}$  and  $\mu^{(1)} = 1$ . The computational results as functions of the film thickness are shown in Fig. 2 by the dashed line for a pure peptide coating and by the lines 1, 2, and 3 for peptide coatings containing the fractions  $\Phi = 0.1, 0.25$ , and  $0.4$  of water, respectively. As is seen in Fig. 2, for pure peptide coating of less than  $130$  nm thickness the fluctuation-induced Casimir pres-

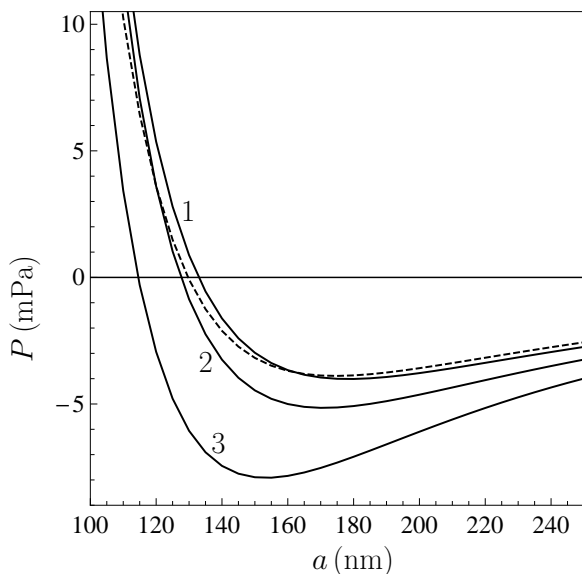


FIG. 2: The Casimir pressures in undoped peptide films deposited on a  $\text{SiO}_2$  substrate are shown as the dashed line for a pure peptide and by the lines 1, 2, and 3 for the films containing  $\Phi = 0.1, 0.25$ , and  $0.4$  fractions of water, respectively, as the functions of film thickness at  $T = 300$  K.

sure becomes positive which makes the film less stable. The same holds for coatings containing  $\Phi = 0.1, 0.25$ , and  $0.4$  fractions of water if they are thinner than  $133, 128$ , and  $115$  nm, respectively. The maximum in magnitude negative Casimir pressures contributing to the coating stability are reached for the film thicknesses  $a = 175, 180, 170$ , and  $155$  nm for the fractions of water in the film  $\Phi = 0, 0.1, 0.25$ , and  $0.4$ , respectively.

Next we consider the peptide coating doped with Au nanoparticles. As in the case of a freestanding film, the  $\Phi = 0.4$  fraction of water in the film before doping is assumed. The computations are again performed by Eq. (1) where now  $\varepsilon^{(1)} = \varepsilon_{\Phi,\beta}^{(p)}$ ,  $\mu^{(1)} = 1$ , and  $\varepsilon^{(2)}$  is the dielectric permittivity of a  $\text{SiO}_2$  substrate. The computational results for the Casimir pressure in peptide coatings are shown in Fig. 3 as functions of the film thickness by the lines 1, 2, and 3 for the doped films with the volume fractions of Au nanoparticles  $\beta = 0.01, 0.03$ , and  $0.05$ , respectively. For comparison purposes, the black line with no number reproduces the line 3 in Fig. 2 showing the Casimir pressure in an undoped peptide coating containing  $\Phi = 0.4$  fraction of water.

As is seen in Fig. 3, the presence of doping widens the range of film thicknesses where the Casimir pressure is negative and makes the minima deeper. Specifically, for the fractions  $\beta = 0.01, 0.03$ , and  $0.05$  of nanoparticles in the peptide coating the pressure changes its sign from negative to positive for film thickness below  $110, 100$ , and  $87$  nm, respectively, to compare with  $115$  nm for an undoped coating (the black line with no number in Fig. 3). The largest magnitudes of the negative Casimir pressure at the points of minimum are  $8.98, 12.63$ , and  $20.0$  mPa reached for the film thicknesses  $a = 150, 135$ , and  $115$  nm, respectively (compared to  $7.91$  mPa reached at  $a = 155$  nm for an undoped peptide coating). Thus, an addition of Au nanoparticles makes the peptide coating

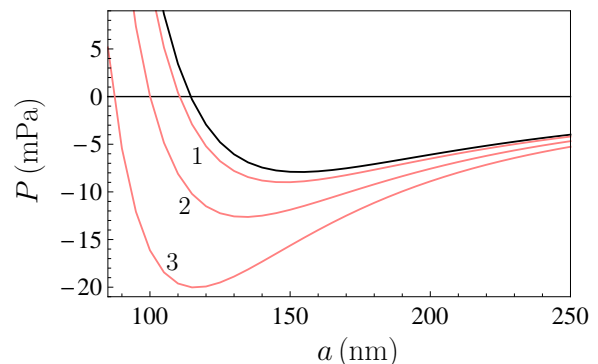


FIG. 3: The Casimir pressures in doped with Au nanoparticles peptide films with  $\Phi = 0.4$  fraction of water deposited on a  $\text{SiO}_2$  substrate are shown by the lines 1, 2, and 3 for the volume fractions of nanoparticles  $\beta = 0.01, 0.03$ , and  $0.05$ , respectively, as the functions of film thickness at  $T = 300$  K. The black line with no number presents similar results for an undoped coating.

more stable over a wider range of film thicknesses.

Finally we consider the case of peptide coatings doped with magnetic nanoparticles which endows the coating with superparamagnetic properties. The computations below are performed for the iron oxide ( $\text{Fe}_3\text{O}_4$ ) magnetite nanoparticles which are often used in ferrofluids [48, 49]. The dielectric permittivity of magnetite along the imaginary frequency axis,  $\varepsilon_m(i\xi)$ , was found in Ref. [49] basing on the measurement data of Ref. [50]. Then, the dielectric permittivity  $\varepsilon_{\Phi,\beta}^{(p)}(i\xi_l)$  of peptide film containing some fraction of water and doped with magnetite nanoparticles was calculated by Eq. (6) where  $\varepsilon_{\text{Au}}$  was replaced with  $\varepsilon_m$ . It was used as  $\varepsilon^{(1)}(i\xi_l)$  in Eq. (1).

The magnetic permeability of peptide coating doped with magnetic nanoparticles deserves special attention. As was mentioned above, the magnetic properties influence the Casimir pressure only through the term of Eq. (1) with  $l = 0$ . This is explained by the fact that at  $T = 300$  K the magnetic permeability drops to unity at much smaller frequencies than  $\xi_1$  [39]. For the static magnetic permeability of peptide coating which is a superparamagnetic system containing the fraction  $\beta$  of single-domain magnetic nanoparticles of radius  $R$  one obtains [51]

$$\mu^{(1)}(0) = 1 + \frac{16\pi^2 R^3 \beta M_s^2}{9k_B T}, \quad (7)$$

where  $M_s \approx 300 \text{ emu/cm}^3 = 3 \times 10^5 \text{ A/m}$  is the saturation magnetization per unit volume for a single nanoparticle of magnetite [52].

We note that according to this equation the magnetic permeability of doped peptide film depends not only on the volume fraction of nanoparticles  $\beta$  but also on their radius. This is not the case for the dielectric permittivity of the same coating which, according to Eq. (6), is completely determined by the value of  $\beta$ . We use the typical value  $R = 5 \text{ nm}$  in below computations. Then, for  $\beta = 0.01, 0.03,$  and  $0.05$  one obtains from Eq. (7) for the static magnetic permeability  $\mu^{(1)}(0) = 1.05, 1.14,$  and  $1.24,$  respectively.

Computations of the Casimir pressure in peptide coatings doped with magnetite nanoparticles were performed by Eq. (1) using the dielectric permittivity and magnetic permeability obtained above as well as the dielectric permittivity of a  $\text{SiO}_2$  substrate  $\varepsilon^{(2)}(i\xi_l)$ . In so doing the  $\Phi = 0.4$  volume fraction of water in the film was assumed. The computational results are shown in Fig. 4 by the lines 1, 2, and 3 as functions of the film thickness for the volume fractions of nanoparticles  $\beta = 0.01, 0.03,$  and  $0.05,$  respectively, at  $T = 300$  K. The black line with no number shows the Casimir pressure in an undoped peptide coating with the same fraction of water. As is seen in Fig. 4, the presence of magnetite nanoparticles in peptide coating again widens the range of film thicknesses where the pressure is negative and makes the minima deeper.

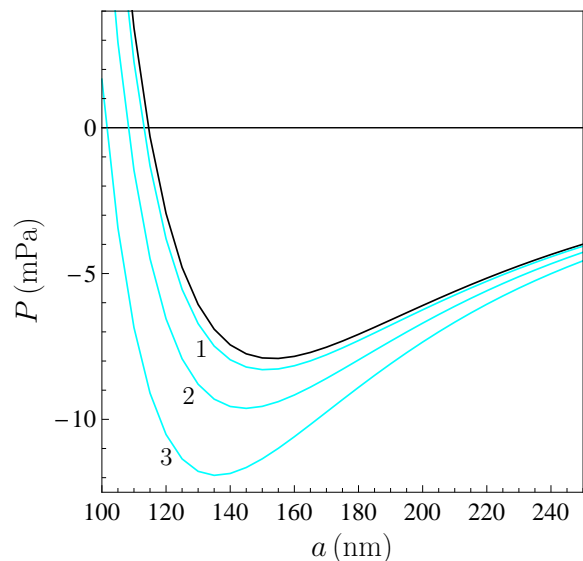


FIG. 4: The Casimir pressures in doped with magnetite nanoparticles peptide films containing  $\Phi = 0.4$  fraction of water deposited on a  $\text{SiO}_2$  substrate are shown by the lines 1, 2, and 3 for the volume fractions of nanoparticles  $\beta = 0.01, 0.03,$  and  $0.05,$  respectively, as the functions of film thickness at  $T = 300$  K. The black line with no number presents similar results for an undoped coating.

Thus, the pressure changes its sign at  $a = 113, 108,$  and  $102 \text{ nm}$  for peptide coatings with  $\beta = 0.01, 0.03,$  and  $0.05,$  respectively (to compare with  $a = 115 \text{ nm}$  for an undoped film). The maximum magnitudes of the Casimir pressure  $8.3, 9.6,$  and  $11.9 \text{ mPa}$  are reached at the extremum points of  $150, 145$  and  $135 \text{ nm}$  for  $\beta = 0.01, 0.03,$  and  $0.05,$  respectively. This should be compared with  $7.91 \text{ mPa}$  at  $a = 155 \text{ nm}$  for an undoped coating. Thus, doping with magnetic nanoparticles results in more stable peptide films possessing superparamagnetic properties.

In the foregoing, we have calculated the fluctuation-induced (Casimir) pressure in thin peptide films and coatings, both undoped and doped with metallic nanoparticles, which makes an impact on the film stability. Estimations show that for films of about  $100 \text{ nm}$  thickness the electromagnetic fluctuations may contribute up to 20% of the total cohesive energy of a film [29, 53] and all the more for thinner films. This adds in importance to the effect of increased stability of peptide films and coatings due to their doping with metallic nanoparticles. Taking into account that stability is the crucial property of a coating, the harnessing of doped peptide films may become beneficial in various applications mentioned above. The proposed doping of a peptide coating with magnetic nanoparticles not only increases the film stability, but makes it superparamagnetic which opens further application areas for bioelectronics, such as in spintronics and magnetic resonance imaging.

The authors were supported by the Peter the Great

Saint Petersburg Polytechnic University in the framework of the Program “5-100-2020”. The work of V.M.M. was partially funded by the Russian Foundation for Basic Research, Grant No. 19-02-00453 A. His work was also partially supported by the Russian Government Program of Competitive Growth of Kazan Federal University.

- 
- [1] A. Ulman, *An Introduction to Ultrathin Organic Films: From Langmuir-Blodgett to Self-Assembly* (Academic Press, London, 1991).
- [2] G. Meller and T. Grasser (eds.), *Organic Electronics* (Springer, Heidelberg, 2010).
- [3] Chun-Yi Lee, Jenn-Chang Hwang, Yu-Lun Chueh, Ting-Hao Chang, Yi-Yun Cheng, and Ping-Chiang Lyu, Hydrated bovine serum albumin as the gate dielectric material for organic field-effect transistors, *Org. Electr.* **14**, 2645 (2013).
- [4] Mingchao Ma, Xinjun Xu, Leilei Shi, and Lidong Li, Organic field-effect transistors with a low driving voltage using albumin as the dielectric layer, *RSC Advances* **4**, 58720 (2014).
- [5] C. D. Dimitrakopoulos and P. R. L. Malenfant, Organic thin film transistors for large area electronics, *Adv. Mater.* **14**, 99 (2002).
- [6] M. Righi, G. L. Puleo, I. Tonazzini, G. Giudetti, M. Cecchini, and S. Micera, Peptide-based coatings for flexible implantable neural interfaces, *Sci. Reports* **8**, 502 (2018).
- [7] T. Guterman and E. Gazit, Toward peptide-based bioelectronics: reductionist design of conductive pili mimetics, *Bioelectron. Med. (Lond.)* **1**, 131 (2018).
- [8] J. Yu, J. R. Horsley, and A. D. Abell, Peptides as Bio-Inspired Electronic Materials: An Electrochemical and First-Principles Perspective, *Acc. Chem. Res.* **51**, 2237 (2018).
- [9] S. S. Panda, H. E. Katz, and J. D. Tovar, Solid-state electrical applications of protein and peptide based nanomaterials, *Chem. Soc. Rev.* **47**, 3640 (2018).
- [10] B. Li, D. T. Haynie, N. Palath, and D. Janisch, Nano-Scale Biomimetics: Fabrication and Optimization of Stability of Peptide-Based Thin Films, *J. Nanosci. Nanotech.* **5**, 2042 (2005).
- [11] P. Fattahi, G. Yang, G. Kim, and M. R. Abidian, A Review of Organic and Inorganic Biomaterials for Neural Interfaces, *Adv. Mater.* **26**, 1846 (2014).
- [12] A. Arul, S. Sivagnanam, A. Dey, O. Mukherjee, S. Ghosh, and P. Das, The design and development of short peptide-based novel smart materials to prevent fouling by the formation of non-toxic and biocompatible coatings, *RSC Advances* **10**, 13420 (2020).
- [13] S. Sharma, R. W. Johnson, and T. A. Desai, Evaluation of the stability of nonfouling ultrathin poly(ethylen glycol) films for silicon-based microdevices, *Langmuir* **20**, 348 (2004).
- [14] M. Natesan and R. G. Ulrich, Protein microarrays, and biomarkers of infection disease, *Int. J. Mol. Sci.* **11**, 5165 (2010).
- [15] C.-K. Chou, N. Jing, H. Yamaguchi, P.-H. Tsou, H.-H. Lee, C.-T. Chen, Y.-N. Wang, S. Hong, C. Su, J. Kameoka, and M.-C. Hung, Rapid detection of two-protein interaction with a single fluorophore by using a microfluidic device, *Analyst* **135**, 2907 (2010).
- [16] H. Chandra, P. J. Reddy, and S. Srivastava, Protein microarrays and novel detection platforms, *Expert Rev. Proteomics* **8**, 61 (2011).
- [17] Pui Mun Lee, Ze Xiong, and John Ho, Methods for powering bioelectronic microdevices, *Bioelectron. Med. (Lond.)* **1**, 201 (2018).
- [18] M. Kardar and R. Golestanian, The “friction” of vacuum, and other fluctuation-induced forces, *Rev. Mod. Phys.* **71**, 1233 (1999).
- [19] R. H. French, V. A. Parsegian, R. Podgornik et al., Long range interactions in nanoscale science, *Rev. Mod. Phys.* **82**, 1887 (2010).
- [20] V. A. Parsegian, *Van der Waals Forces: A Handbook for Biologists, Chemists, Engineers, and Physicists* (Cambridge University Press, Cambridge, 2005).
- [21] M. Bordag, G. L. Klimchitskaya, U. Mohideen, and V. M. Mostepanenko, *Advances in the Casimir Effect* (Oxford University Press, Oxford, 2015).
- [22] G. L. Klimchitskaya, U. Mohideen, and V. M. Mostepanenko, The Casimir force between real materials: Experiment and theory, *Rev. Mod. Phys.* **81**, 1827 (2009).
- [23] L. M. Woods, D. A. R. Dalvit, A. Tkatchenko, P. Rodriguez-Lopez, A. W. Rodriguez, and R. Podgornik, Materials perspective on Casimir and van der Waals interactions, *Rev. Mod. Phys.* **88**, 045003 (2016).
- [24] E. M. Lifshitz and L. P. Pitaevskii, *Statistical Physics, Pt. II* (Pergamon Press, Oxford, 1980).
- [25] V. A. Parsegian and B. W. Ninham, Application of the Lifshitz theory to the calculation of van der Waals forces across thin lipid films, *Nature* **224**, 1197 (1972).
- [26] S. Nir, Van der Waals interactions between surfaces of biological interest, *Progr. Surf. Sci.* **8**, 1 (1976).
- [27] C. M. Roth, B. L. Neal, and A. M. Lenhoff, Van der Waals interactions involving proteins, *Biophys. J.* **70**, 977 (1996).
- [28] Bing-Sui Lu and R. Podgornik, Effective interactions between fluid membranes, *Phys. Rev. E* **92**, 022112 (2015).
- [29] M. A. Baranov, G. L. Klimchitskaya, V. M. Mostepanenko, and E. N. Velichko, Fluctuation-induced free energy of thin peptide films, *Phys. Rev. E* **99**, 022410 (2019).
- [30] E. N. Velichko, M. A. Baranov, and V. M. Mostepanenko, Change of sign in the Casimir interaction of peptide films deposited on a dielectric substrate, *Mod. Phys. Lett. A* **35**, 2040020 (2020).
- [31] Jinmao Yan, Yunxiang Pan, A. G. Cheetham, Yi-An Lin, Wei Wang, Honggang Cui, and Chang-Jun Liu, One-Step Fabrication of Self-Assembled Peptide Thin Films with Highly Dispersed Noble Metal Nanoparticles, *Langmuir* **29**, 16051 (2013).
- [32] G. L. Klimchitskaya and V. M. Mostepanenko, Observability of thermal effects in the Casimir interaction with graphene-coated substrates, *Phys. Rev. A* **89**, 052512 (2014).
- [33] G. L. Klimchitskaya and V. M. Mostepanenko, Casimir free energy of metallic films: Discriminating between Drude and plasma model approaches, *Phys. Rev. A* **92**, 042109 (2015).
- [34] G. L. Klimchitskaya and V. M. Mostepanenko, Casimir and van der Waals energy of anisotropic atomically thin metallic films, *Phys. Rev. B* **92**, 205410 (2015).
- [35] G. L. Klimchitskaya and V. M. Mostepanenko, Casimir free energy and pressure for magnetic metal films, *Phys.*

- Rev. B **94**, 045404 (2016).
- [36] G. L. Klimchitskaya and V. M. Mostepanenko, Characteristic properties of the Casimir free energy for metal films deposited on metallic plates, *Phys. Rev. A* **93**, 042508 (2016).
- [37] G. L. Klimchitskaya and V. M. Mostepanenko, Low-temperature behavior of the Casimir free energy and entropy of metallic films, *Phys. Rev. A* **95**, 012130 (2017).
- [38] G. L. Klimchitskaya and V. M. Mostepanenko, Casimir free energy of dielectric films: Classical limit, low-temperature behavior and control, *J. Phys.: Condens. Matter* **29**, 275701 (2017).
- [39] B. Geyer, G. L. Klimchitskaya, and V. M. Mostepanenko, Thermal Casimir interaction between two magnetodielectric plates, *Phys. Rev. B* **81**, 104101 (2010).
- [40] A. Gennadios (ed.), *Protein-Based Films and Coatings* (CRC Press, Boca Raton, 2002).
- [41] N. Gontard and S. Ring, Edible wheat gluten film: Influence of water content on glass transition temperature, *J. Agric. Food Chem.* **44**, 3474 (1996).
- [42] G. Löffler, H. Schreiber, and O. Steinhauser, Calculation of the Dielectric Properties of a Protein and its Solvent: Theory and a Case Study, *J. Mol. Biol.* **270**, 520 (1997).
- [43] P. Adhikari, A. M. Wen, R. H. French, V. A. Parsegian, N. F. Steinmetz, R. Podgornik, and W.-Y. Ching, Electronic Structure, Dielectric Response, and Surface Charge Distribution of RGD (1FUV) Peptide, *Sci. Reports.* **4**, 5605 (2014).
- [44] L. Bergström, Hamaker constant of inorganic materials, *Adv. Coll. Interface Sci.* **70**, 125 (1997).
- [45] D. B. Hough and L. H. White, The calculation of Hamaker constant from Lifshitz theory with application to wetting phenomena, *Adv. Coll. Interface Sci.* **14**, 3 (1980).
- [46] *Handbook of Optical Constants of Solids*, ed. E. D. Palik (Academic, New York, 1985).
- [47] A. H. Sihvola, *Electromagnetic Mixing Formulas and Applications* (The Institution of Electrical Engineers, London, 1999).
- [48] T. Guo, X. Bian, and C. Yang, A new method to prepare water based Fe<sub>3</sub>O<sub>4</sub> ferrofluid with high stabilization, *Physica A: Stat. Mech. Applic.* **438**, 560 (2015).
- [49] G. L. Klimchitskaya, V. M. Mostepanenko, E. K. Nepomnyashchaya, and E. N. Velichko, Impact of magnetic nanoparticles on the Casimir pressure in three-layer systems, *Phys. Rev. B* **99**, 045433 (2019).
- [50] A. Schlegel, S. F. Alvarado, and P. Wachter, Optical properties of magnetite (Fe<sub>3</sub>O<sub>4</sub>), *J. Phys. C: Solid State Phys.* **12**, 1157 (1979).
- [51] S. V. Vonsovskii, *Magnetism* (Wiley, New York, 1974).
- [52] S. van Berkum, J. T. Dee, A. P. Philipse, and B. E. Erné, Frequency-dependent magnetic susceptibility of magnetite and cobalt ferrite nanoparticles embedded in PAA hydrogel, *Int. J. Mol. Sci.* **14**, 10162 (2013).
- [53] I. Boinovich and A. Emelyanenko, Wetting and surface forces, *Adv. Coll. Interface Sci.* **165**, 60 (2011).